High Resolution Micro-Pirani Pressure Sensor with Transient Response Processing and Time-Constant Evaluation

Olivier Legendre, Hervé Bertin, Olivier Garel, Ming Zhang, Hervé Mathias, Souhil Megherbi, Jérôme Juillard, Frédérick Mailly

High-Resolution Micro-Pirani Pressure Sensor With Transient Response Processing and Time-Constant Evaluation

Olivier Legendre, Hervé Bertin, Olivier Garel, Ming Zhang, Hervé Mathias, Souhil Mergherbi, Jérôme Juillard, and Frédérick Mailly

Abstract—**A micro-Pirani pressure sensor, which consists of a pressure-dependent thermoresistance gauge, is traditionally exploited using a steady-state resistance measurement. Any signal variation occurs over an offset voltage due to the imperfection of the device, which affects the sensor's sensitivity. This paper presents, for the first time, an experimental investigation of a micro-Pirani gauge based on its dynamic behavior when heated by a current step. Such processing magnifies the pressure dependence of the gauge's signal by eliminating the constant offset influences on the measurement. Furthermore, a first-order low-pass filter step response identification of the experimental transient signal strongly reduces the noise influence on the measurement. Furthermore, such identification enables a direct calculation of the time constant. This paper investigates the pressure measurement based on the time-constant evaluation, which provides a range of measurement and a maximal sensitivity significantly shifted toward the atmospheric pressure compared to that of a traditionally processed Pirani gauge. The heating step, the recording of the transient response signal, and its digital postprocessing can be easily achieved by a small-sized controller. The proposed system provides a substantial performance enhancement of the micro-Pirani pressure sensor.**

Index Terms—**Microelectromechanical devices, microsensors, Pirani gauges, pressure gauges, system identification.**

I. Introduction

FOR the last twenty years, sensors capabilities have been considerably modified with the emergence of Micro-Electro-Mechanical-Systems (MEMS) technologies. Recent research on micro-sensor chips has focused on monolithic sensor integration which allows minimizing the micro-system size and simplifying the packaging required for system-level assembly. It is now possible to get heterogeneous systems using standard CMOS technologies, including the sensor transducer and its own readoult electronics. The integration of the latter in the vicinity of the sensing part enables the lowering of production cost and the enhancement of sensor performance mainly because of noise reduction.

Traditionally used for vacuum monitoring while heated by a constant biasing current, a micro-Pirani sensor converts a pressure variation of the surrounding air into a resistance variation of the heated gauge, since the thermal conductivity of the air is pressure dependent, which affects the steady state temperature of the gauge. Usually the transduction is realized using a gauge made of a material having a high Temperature Coefficient of Resistance (TCR) which converts a temperature variation into a resistance variation. The steady state temperature of the gauge is proportional to the heating power (in Watt), so are the gauge's pressure dependent resistance variations, *on a first order*. As a result, the gauge's sensitivity is proportional to the heating power, which is proportional to the square value of the heating current. In the case of low-power consumption requirement, which is common place for micro-systems, the available current to be fed into the gauge is limited which affects both of the device's sensitivity and resolution, since the signal-to-noise ratio is proportional to the device sensitivity.

The resistance variations are monitored by a conditioning and measurement circuitry [1]–[4]. When the micro-Pirani is put inside a resistor-bridge and when the bridge is initially perfectly balanced, the output of the bridge is mainly proportional to the resistance variation of the gauge. However, many imperfections of the real device can introduce performance losses. For example, the unbalancing of the bridge due to devices dimensions dispersion or a reference voltage drift, induce an offset voltage at the output which affects the resistance variation measurement. This problem is usually dealt with dynamical balancing of the bridge through a monitored resistor self-test method [5], [6] which consists on the self calibrating of the device. These self calibrating methods are producing an incremental counter-offset which can not eliminate it perfectly due to the quantization error and the range of the offset rejection is also limited.

On other hand, much recent achievements in micro-Pirani device lead to provide micro-sensor allowing pressure measurement in the atmospheric pressure range [1], [2], [4]. Thanks to the micromachining possibilities, this could be achieved in reducing the thickness of the gas layer surrounding the sensor in the sub-micrometer range in order to shift the range of measurement towards the 1000 mbar range.

Manuscript received October 21, 2011; revised December 13, 2011; accepted December 18, 2011. The associate editor coordinating the review of this paper and approving it for publication was Dr. M. Nurul Abedin.

O. Legendre, H. Bertin, O. Garel, M. Zhang, H. Mathias, and S. Mergherbi are with MiNaSys, Université Paris-Sud, Orsay 91400, France (e-mail: legendre.o@gmail.com; herve.bertin@u-psud.fr; olivier.garel@u-psud.fr; ming.zhang@u-psud.fr; herve.mathias@u-psud.fr; souhil.megherbi@u-psud.fr).

J. Juillard is with E3S, SupElec, Gif-sur-Yvette 91192, France (e-mail: jerome.juillard@supelec.fr).

F. Mailly is with the Montpellier Laboratory of Computer Science, Robotics, and Microelectronics, University of Montpellier, Montpellier, France (e-mail: frederick.mailly@lirmm.fr).

These previous sensor are working using the steady state signal of the Pirani gauge.

On the opposite, a recent study [7] observed that the transient response of a *macro*-Pirani gauge features a significant sensitivity inside the 30 mbar to 1000 mbar range. The gauge used was initially designed for measuring high vacuum since the gaseous layer was 16 mm thick. As it will be seen further, the steady state signal of such a gauge would be non-sensitive inside this pressure range, whereas the transient signal of this gauge became pressure sensitive.

This paper investigates for the first time the experimental processing of the transient response of a micro-Pirani gauge. One a first hand, the transient response helps to provide high resolution pressure measurements from an offset-free signal, because it enables the measurement of both the gauge resistance when it is cold (initial state) and when it is heated (steady state). Using a digital sampling and a recording of the transient response of the output of the bridge, any offset occurring can thus be eliminated by digital post-processing thus magnifying the unbalanced bridge sensitivity and features a self calibrating of the device. A digital identification of the sensor's transient response can be performed on the offset-free signal to further enhance the measurement resolution. This paper particularly investigates the use of a fast identification technique based on the use of an Auto-Regressive Moving Average (ARMA) model to get a good noise resolution at a low hardware cost. The investigated post-processing methods are compared altogether at the end.

On a second hand, thanks to the ARMA identification of the transient response, we investigate a novel pressure measurement based on the sensor's transient response in order to reach pressure measurement near the atmospheric pressure.

This paper is organized as follow: first, we describe the considered sensor, its conditioning and its transient response to a current step (Part II). Following the theoretical description of the performance enhancement obtained with the ARMA filter (Part III), we will present and discuss the obtained experimental results (Part IV) before a final conclusion (Part VI).

II. Sensor Description

The pressure measurement is performed using a micro-wire (the micro-Pirani gauge) which consists on a 0.7 μm thick layer of polycrystalline silicon, covered by a 0.5 μm thick layer of silicon oxide and by a 1.5 μm thick layer of nitride passivation layer respectevelly. The gauge length and width are 1 mm and 40 μm. The gauge is released from the silicon substrate and it is suspended over a $d = 300$ μm thick gaseous layer as shown on "Fig. 1". Biased by an electrical current, though the conductive polycrystalline layer, the micro-wire acts as a heat source due to Joule effect. Besides substantial thermal losses at the anchors of the micro-wire, losses occur across the surrounding gaseous layer by conduction, convection and radiation. These losses result in a lowering of the gauge temperature which affects its resistance. As a matter of fact, the micro-wire will grow hotter as the pressure in the surrounding atmosphere is lowered.

This section will first summarize the key sources of error of a micro-Pirani gauge when it is traditionally processed.

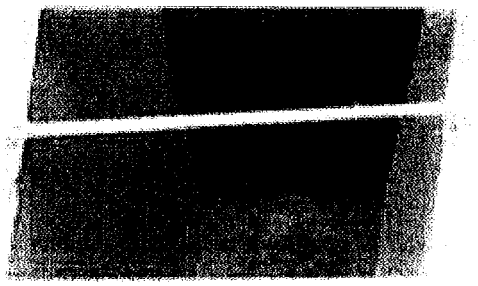

Fig. 1. SEM image of the micro-Pirani gauge. It consists of a micro-wire suspended over a deep gaseous layer. Heated by a constant electrical current, its temperature depends on the gasous layer thermal conductivity, which is pressure dependent.

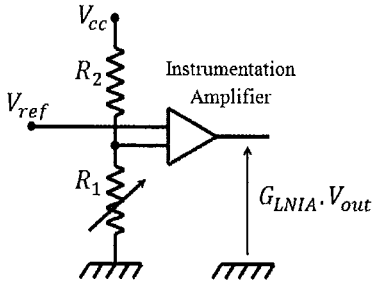

Fig. 2. Pirani gauge (R_1) within the half Wheatstone bridge. G_{LNIA} is the gain of the low noise instrumentation amplifier.

In a second part a theoretical background of the transient response of the sensor will be shortly given.

A. Sources of Error in the Case of a Steady State Measurement

As shown in "Fig 2", the pressure dependent resistor (R_1) is placed inside a resistor bridge, completed by a reference resistor (R_2) which is the same micro-wire except that it is not suspended over a gaseous layer and is directly in thermal contact with the substrate. A Low Noise Instrument Amplifier (LNIA) with gain G_{LNIA} enables the reading of slight changes of the voltage divider's output formed by R_1 and R_2.

The formula for the output voltage V_{out} is given by

$$V_{out} = \left(V_{cc} \cdot \frac{R_1}{(R_1 + R_2)} - V_{ref} \right) \cdot G_{LNIA} \qquad (1)$$

and the resistor bridge is said perfectly balanced if both $R_1 = R_2$ and $V_{ref} = V_{cc}/2$, so that the output voltage is null. One may notice here that the output signal of this type of bridge is strongly independent upon the ambient temperature variations if R_1 and R_2 are fabricated with the same material (i.e. their TCR is the same).

Assuming that the reference resistor (R_2) is in perfect thermal contact with the substrate (i.e. its temperature is set at ambient temperature and it will not be heated by the current feeding), and that the bridge is initially perfectly balanced, the steady state resistance variation due to the heating $\delta R_{1_{steady}} \ll R_1$ results in an output voltage

$$V_{out,balanced} = V_{cc} \cdot \frac{\delta R_{1_{steady}}}{R_1 + R_2 + \delta R_{1_{steady}}} \cdot G_{LNIA}. \qquad (2)$$

The half Wheatstone bridge is in fact very difficult to balance perfectly. First, the fabrication of the micro-sensor requires the transducer resistor (R_1) to be released from the substrate, which may slightly narrow its resistive layer during the etching process and thus can change its nominal resistance value, leading to a non-negligible mismatch between the two resistors δR_m. Second, an unexpected offset δV_{ref}, due to a drift of the reference voltage or the input offset of the LNIA would also lead to an extra offset voltage at the circuit output. The overall offset voltage V_{off} would be given by, assuming $\delta R_m \ll R_1$

$$V_{off} = \left(V_{cc} \cdot \frac{\delta R_m}{R_1 + R_2 + \delta R_{1_{steady}} + \delta R_m} + \delta V_{ref} \right) \cdot G_{LNIA}. \quad (3)$$

This resulting offset voltage may be much higher than the measurement voltage calculated in (2), especially if the power consumption allowed to the gauge heating is limited (i.e. $\delta R_{1_{steady}}$ is very low). This is a major source of error which affects the correctness of the pressure measurement.

Another source of error is the intrinsic noise in the sensor's output signal which is governed by both thermal noise of the resistive parts of the bridge and by the noise sources of the amplifier. These sources of error will affect the measurement resolution.

B. Transient Response

Since this study investigates the transient response of the pressure gauge as an easy way to achieve a rejection of the offset voltage, the following part will give a theoretical background concerning the transient response of the sensor.

When operating in vacuum, thermal transfer by convection can easily be neglected since it is mainly proportional to pressure. Lowering the heating power consumption of the gauge being a major concern of this work, the heating of the micro-wire will be kept low enough so that radiant losses can be neglected. The remaining sensor's thermal losses are hence principally due to thermal conduction at the anchor and across the surrounding gaseous layer, mainly towards the substrate below acting as a heat sink kept at the ambient temperature T_a. This thermal loss is strongly pressure dependent inside a bounded range of pressure and is the key physical principle behind the (micro-) Pirani gauge. The following part will shortly describe the transient heat conduction problem for the micro-wire with self heating due to Joule effect.

The excess-temperature in the system $\theta(r,t)$ over the ambient temperature T_a satisfies of the following heat conduction boundary value problem:

$$\rho(\boldsymbol{r}) c_p(\boldsymbol{r}) \frac{\partial \theta(\boldsymbol{r},t)}{\partial t} = \nabla \left[k(\boldsymbol{r}) \cdot \nabla \theta(\boldsymbol{r},t) \right] + g(\boldsymbol{r},t) \quad (4.1)$$

$$\theta(\boldsymbol{r},t) \text{ continuous} \quad (4.2)$$

$$k(\boldsymbol{r}) \cdot \nabla \theta(\boldsymbol{r},t) \text{ continuous} \quad (4.3)$$

$$\theta(\boldsymbol{r},t) = 0 \text{ if } \boldsymbol{r} \text{ is inside the silicon substrate} \quad (4.4)$$

$$\theta(\boldsymbol{r},t) = 0 \text{ if } \theta t \leq 0 \quad (4.5)$$

where ρ, c_P and k are respectively the density (in $\mathrm{Kg.m^{-3}}$), the specific heat (in $\mathrm{J.Kg^{-1}.K^{-1}}$), and the thermal conductivity (in $\mathrm{W.K^{-1}.m^{-1}}$) at the space coordinate $\boldsymbol{r}$, t the time and g the heat generation (in $\mathrm{W.m^{-3}}$).

Given the shape of the micro-wire, one may rewrite (4.1) in the following form:

$$\rho_i c_{p_i} \cdot \frac{\partial \theta_i(\boldsymbol{r},t)}{\theta t} = k_i \nabla^2 \theta_i(\boldsymbol{r},t) + g_i(t) \quad (5)$$

where $i = 1$ if the coordinate r is inside the micro-wire medium, $i = 2$ if r is inside the gaseous medium, ∇^2 being the three dimensional Laplace differential operator. The heat generation inside the micro-wire is given by $g_1 = R_1.i(t)^2/vol, i(t)$ being the current (in A) driven alongside the micro-wire and vol its volume (in $\mathrm{m^3}$) and $g_2 = 0$.

The transient resistance variation of the gauge $\delta R(t)$ is given by

$$\delta R_1(t) = R_1 \cdot \alpha(T_a) \langle \theta_1(r,t) \rangle \quad (6)$$

where $\alpha(T_a)$ (in $\mathrm{K^{-1}}$), is the TCR of the gauge evaluated at the ambient temperature T_a (in K) and $\langle \theta_1(r,t) \rangle$ the mean value of the excess temperature inside the micro-wire (in K). It can be shown that when the gauge is heated by a step current $i(t \leq 0) = 0$ A and $i(t > 0) = I_0$, the transient resistance variation $\delta R_1(t)$ is of the following general form:

$$\delta R_1(t) = R_1 \cdot I_0^2 \sum_{n=0}^{\alpha} G_n \left(1 - \exp\left(-\frac{t}{\beta_n} \right) \right) \quad (7.1)$$

$$0 < \beta_1 < \beta_2 < \cdots < \beta_n < \cdots \quad (7.2)$$

where β_n and G_n are sets of parameters that are all pressure dependent. The interested reader will find more details concerning the calculation of G_n and β_n and the heat conduction equation studies in [8] which is far beyond the realm of this paper. However, is has to be notified that the transient signal of the heated micro-wire is a linear combination of eigen-mode just like it is for vibrating strings, except that the partial derivative problem is of a different nature. For the micro-Pirani gauge used in this study, the amplitude of the first mode G_1 is much greater than the other one, so that the transient resistance variation $\delta R_1(t)$ given by (7) could be simplified by the following:

$$\delta R_1(t) \cong \delta R_{1_{steady}} \left(1 - \exp\left(-\frac{t}{\beta} \right) \right) \quad (8)$$

where $\delta R_{1_{steady}}$ is mainly proportional to $R_1 I_0^2$, besides of its pressure dependence.

The steady state is reached when $\partial \theta(r,t)/\partial t = 0$, so that (5) becomes

$$k_i \nabla^2 \theta_i(r, t \to \alpha) + g_i(t) = 0 \quad (9)$$

and the only physical parameter of (9) which is pressure dependent becomes the thermal conductivity of the surrounding gas k_2. Its variations with respect to pressure dependence are shown in "Fig. 3". The dependence of k_2 with respect to the pressure is of the following form:

$$k_2 = \frac{a_1}{\sqrt{T_a}} \frac{P \cdot P_t}{(P + P_t)} \cdot d \quad (10.1)$$

$$P_t = \frac{a_2}{d} \quad (10.2)$$

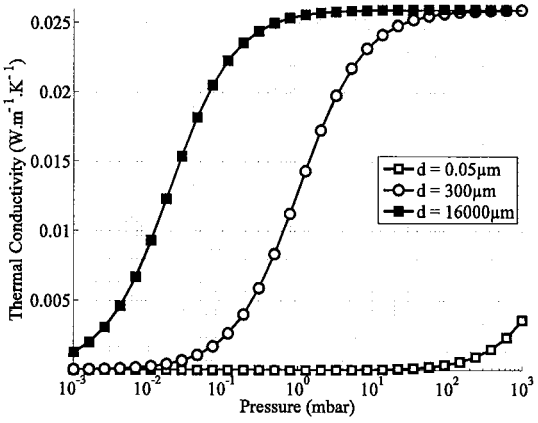

Fig. 3. Gaseous thermal conductivity k_2 of air versus pressure at $T_a = 300$ K for different values of the gaseous layer thickness $d = 50$ nm [3], 300 μm, 16 mm [7]. The transition pressure in our case ($d = 300$ μm) is $d = 104$ $Pa = 1.03$ mbar.

where p and P_t are respectively the ambient pressure and the transition pressure (in Pa), d is the thickness of the gaseous layer separating the heated resistance and the heat sink, $a_1 = 14.33$ W/m^2/K$^{1/2}$/Pa and $a_2 = 3.139\ 10^{-2}$ Pa.m being thermodynamics constant detailed in [1], [2]. The transition pressure P_t gives the pressure at which the Pirani gauge is the most sensitive, explaining that reducing the gas layer thickness shift the sensor's range of measurement toward the atmospheric pressure.

As a matter of fact, a Pirani gauge is based upon the pressure dependence of its steady state resistance variation $\delta R_{1steady} = \delta R(t \rightarrow \infty)$. Since $\delta R_1(t)$ is varying from 0 to $\delta R_{1steady}$, it is possible to use the transient response starting value of the bridge output, which is not pressure dependent, as a signal reference for the measurement of $\delta R_{1steady}$, which is strongly pressure dependent.

This second section introduced that a strong common mode rejection would be necessary to achieve measurement correctness while measurement resolution is dependent upon noise rejection. It also put forwards a theoretical background concerning the physical principles involved in both the transient response of the sensor and the pressure dependence of its steady state.

III. Performance Enhancement

This section deals with the signal processing used to improve both the correctness and resolution of the pressure measurement. The first part details how the transient response is an easy way to achieve the expected common mode rejection. Thanks to the transient response shape of the sensor, the second part shows how an ARMA modeling identification of the digitalized sensor's response enables a powerful noise rejection while improving the common mode rejection.

In order to achieve such a processing, the half Wheatstone bridge is followed by a 16-bit Analog-to-Digital Converter (ADC). The analog to digital conversion of $V_{out\,LNA}(t)$, noted $V_{out}[n]$, is next made at the sample frequency $f_S = 5.12$ kHz, where the ADC full scale is $V_{max} - V_{min}$ and the least significant bit is $LSB = (V_{max} - V_{min})/2^{16}$.

A. Common Mode Rejection

A first post-processing method consists of subtracting the value of the first recorded point to the recorded digital sensor's response $V_{out}[n]$, giving

$$\overline{V_{out}[n]} = V_{out}[n] - V_{out}[1] \tag{11}$$

which allows a powerful rejection of the nominal offset from the recorded signal.

An easy way to achieve the measurement of the pressure P is to use the mean value (i.e. the integration) of the previous signal since it provides easily a substantial noise rejection, giving:

$$\begin{aligned} V_A(P) = \langle \overline{V_{out}[n]} \rangle &= \frac{1}{N} \sum_{n=1}^{N} \overline{V_{out}[n]} \\ &= \langle V_{out}[n] \rangle - V_{out}[1] \end{aligned} \tag{12}$$

where N is the number of samples recorded.

Assuming that the noise affecting the transient response follows a white noise distribution, and that $N \gg 1$, one may calculate that the standard deviation of $V_A(P)$, is

$$\begin{aligned} std(V_A(P)) &= std(V_{out}[1]) + std(\langle V_{out}[n] \rangle) \\ &= std(V_{out}[1]) \cdot \left(1 + \frac{1}{\sqrt{N}}\right) \end{aligned} \tag{13}$$

which is dominated by $std(V_{out}[1])$, due to the subtracting of $V_{out}[1]$ from the recorded signal $V_{out}[n]$ in (12).

B. Common Mode Rejection Improvement

According to the previous section, the resolution would be enhanced if the common mode rejection is performed using a subtracting term whose standard deviation is lower than $std(V_{out}[1])$, null at best. Since the transient part of the gauge response is very similar to the step response of a low-pass filter, see (8), the following post-processing method consists of performing an identification of $V_{out}[n]$ with the step response of an ARMA modeling. An ARMA modeling identification enables the reconstruction of an estimation of $V_{out}[n]$ from a very small set of parameters. It also enables a powerful noise rejection. Hence, a subtracting value with a low standard deviation, can be found, improving the measurement resolution, which is detailed below.

Due to (8), the signal $V_{out}[n]$ can easily be approximated by the following expression:

$$V_{out}[n] \cong G(P) \cdot \left(1 - \exp\left(-\frac{t[n]}{\beta(P)}\right)\right) + V_{off} \tag{14}$$

which is the step response of a first order low-pass filter (i.e. a low pass RC filter), whose gain $G(P)$ and time constant $\beta(P)$ are both pressure dependent, added to an offset value V_{off}.

The idea here is to get the corresponding digital filter using an ARMA modeling from a parametric signal identification technique. The ARMA modeling is computed using the *Steiglitz-McBride* algorithm [9], which calculates the transfer function $H(Z)$ leading to the output signal from $V_{out}[n]$ an input signal $X[n]$, where $X[n]$ is a $1 \times N$ vector filled with 1

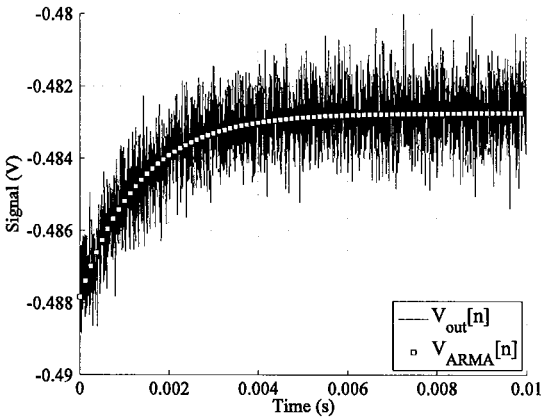

Fig. 4. Illustrative example of the transient signal ($V_{\text{out}}[n]$) post-processing of ARMA modeling identification with the step response of a low pass filter ($V_{\text{ARMA}}[n]$). Such signal processing enables a powerful noise rejection.

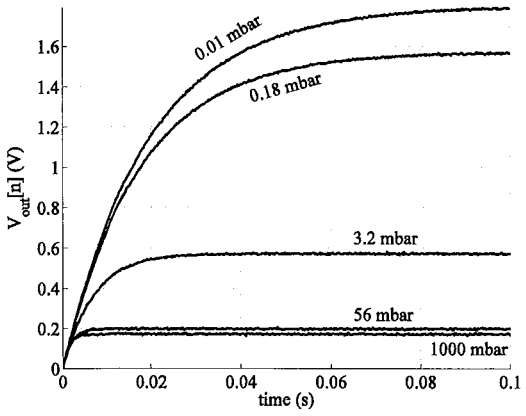

Fig. 5. Experimental analog sensor's transient response versus time, for different values of the pressure. Transient signal is offset free using (11), and it is not processed with the ARMA algorithm.

only, figuring the input step signal. The most general form of $H(Z)$ is

$$H(z) = \frac{B(z)}{A(z)} = \frac{b(1) + b(2)z^{-1} + b(3)z^{-2} + b(4)z^{-3} + \cdots}{a(1) + a(2)z^{-1} + a(3)z^{-2} + a(4)z^{-3} + \cdots} \quad (15)$$

where $B(Z)$ and $A(Z)$ are the vectors containing the parameters calculated for the identification of $V_{out}[n]$. The *Steiglitz-McBride* algorithm has been specifically chosen due to its low time computing performance. Furthermore, using an approximate value of $H(Z)$ as an initial condition enables solving only linear equations, without performing any matrix inversion, which is usually too computationally intensive.

Due to (8), the ARMA model is chosen to be of the lowest possible order, hence

$$H(z) = \frac{B(z)}{A(z)} = \frac{b(1) + b(2)z^{(-1)}}{1 + az^{-1}}. \quad (16)$$

The reconstructed transient signal, $V_{ARMA}[n]$, is calculated recursively as follows:

$$V_{ARMA}[n] = b(1) + b(2) - a \cdot V_{ARMA}[n-1] \quad (17.1)$$

$$V_{ARMA}[1] = b(1) \quad (17.2)$$

as pictured in "Fig. 4". $V_{ARMA}[n]$ being an estimation of the recorded signal $V_{out}[n]$, an offset cancellation, such as (12), can be achieved using a well chosen subtracting value. The less dispersed part of $V_{ARMA}[n]$ is its steady level (i.e. the right-end side of $V_{ARMA}[n]$ in "Fig. 4"), where

$$std(V_{ARMA}[N]) \gtrsim std(V_{out}[1]) \cdot \frac{1}{\sqrt{N}} \quad (18)$$

as demonstrated in [9], so that

$$\overline{V_{ARMA}[n]} = V_{ARMA}[n] - V_{ARMA}[N]. \quad (19)$$

Accordingly to (12), the pressure measurement is based on

$$(V_B(P)) = \langle \overline{V_{ARMA}[n]} \rangle = \langle V_{ARMA}[n] \rangle - V_{ARMA}[N] = \langle V_{out}[n] \rangle - V_{ARMA}[N] \quad (20)$$

TABLE I
EXPERIMENTAL PARAMETERS

Symbol	Quantity	Value
f_s	sample frequency	5120 Hz
N	number of samples	512 samples
V_{cc}	bridge biasing voltage	2.5 V
V_{off}	offset range	-1.5 V $\rightarrow$ $+1.5$ V
V_{min}, V_{max}	ADC reference voltage	-3.5 V, $+3.5$ V
$R_1 = R_2$	nominal bridge resistance	3989 Ω
G_{LNIA}	LNIA gain	100
I_0	heating current	312 μA
P	pressure range	0.01 mbar $\rightarrow$ 1000 mbar
T_a	ambient temperature	300 K

since $\langle V_A RMA[n] \rangle = \langle V_o ut[n] \rangle$, as demonstrated in [9]. The expected dispersion of the measurement becomes

$$std(V_B(P)) = std(V_{ARMA}[N]) + std(\langle V_{out}[n] \rangle) \gtrsim \frac{2.std(V_{out}[n])}{\sqrt{N}}. \quad (21)$$

The expected yield ξ on the resolution with respect to that common mode rejection compared to the previous section would be

$$\xi = \frac{std(V_A(P))}{std(V_B(P))} \lesssim \frac{1 + \sqrt{N}}{2}. \quad (22)$$

IV. RESULTS

This section will experimentally demonstrate that the offset cancellation based on the ARMA modeling identification of the transient response of a micro-Pirani gauge provides a significant improvement of the pressure measurement resolution compared to the offset cancellation based on the transient response digitalization only.

We first decided to record a large set of our sensor's transient responses, samples being shown in "Fig. 5", with respect to experimental parameter given in "Table I", in order

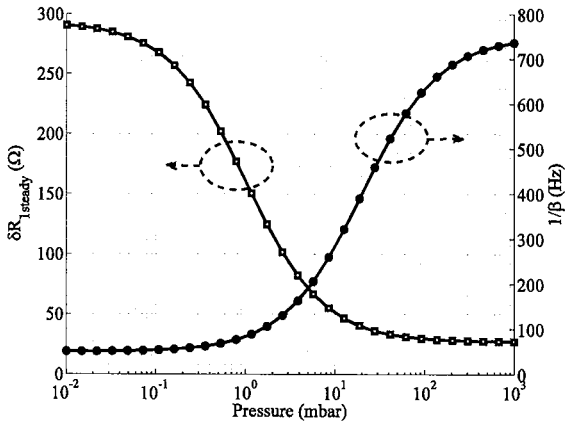

Fig. 6. Steady state resistance variation $\delta R_{1_{steady}}$ versus pressure P (white square, left axis) and cut-off frequency $1/\beta$ versus pressure P (black dot, right axis).

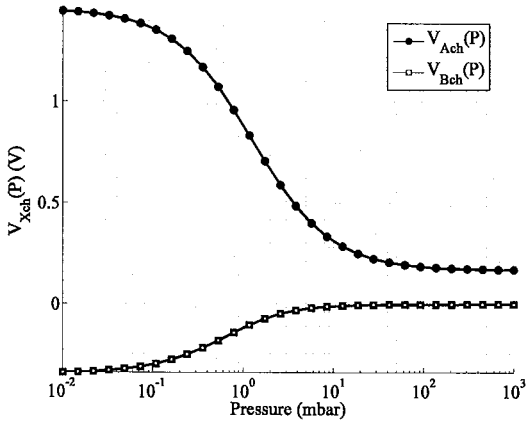

Fig. 7. Sensor's characteristic curves versus pressure.

to extract an experimental physical modeling of our micro-Pirani gauge behavior versus the pressure.

The pressure dependence of both $\delta_{R_{1steady}}$ and $1/\beta$, from (8), are extracted from recorded data with a non-linear interpolation tools of a Matlab platform, which are shown in "Fig. 6".

In order to compare the performance of the two post-processing methods previously described, the characteristic curves $V_{Ach}(P) = \langle V_A(P) \rangle$ and $V_B(P) = \langle V_B(P) \rangle$ are obtained from a large set of measurement $V_A(P)$ and $V_B(P)$ at a single value of the pressure P. They are calculated from (12) and (19) respectively, at a given value of the pressure P and from a large set of $\delta R_m = -3\%R_2 \rightarrow +3\%R_2$ and $\delta V_{ref} = -3\%V_{ref} \rightarrow +3\%V_{ref}$. Since $V_X(P)$, $X = A$ or B, are both monotonous curves, it is possible to get their reciprocal curve $P_X(V)$, which returns the pressure measured from a given measurement value of $V_X(P)$, as is shown in "Fig. 7 ".

The pressure measurement resolution has been evaluated using offline computation based on the gauge's transient response modeling previously described on which an input equivalent noise pattern is added so as to get a signal-to-noise

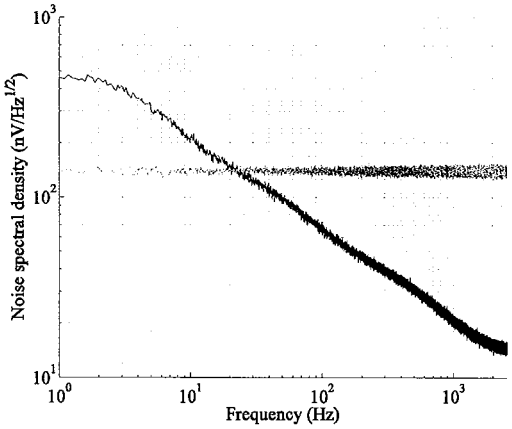

Fig. 8. $1/f$ noise distribution (black) and white noise distribution (gray) spectral density versus frequency. These two distributions are used in order to estimate the sensor's measurement resolution.

TABLE II
$1/f$ NOISE ARMA MODELING FILTER
$H(Z) = \sum_{i=1}^{4} b(i)z^{1-i} / \sum_{i=1}^{4} a(i)z^{1-i}$

i	$a(i)$	$b(i)$
1	1	0.049922
2	−2.4949	−0.095993
3	2.0172	0.050613
4	0.52219	0.0044088

ratio as close as possible to the experimental sensor's transient response.

The input equivalent noise pattern, shown in "Fig. 8" is made of a $1/f$ noise pattern and a white noise pattern. The $1/f$ noise is generated from a filtered white noise of sample frequency F_S. The ARMA model of this filter is given in "Table II". The input white noise, with a unity standard deviation, is applied long enough to provide a significant amount of low frequencies. Next, to model the LNIA noise, this $1/f$ noise distribution is added to a white noise with a spectral density of 140 nV/$\sqrt{Hz}$. The $1/f$ noise is previously amplified so that the $1/f$ corner is at 20 Hz, which is quite close to the $1/f$ corner of the LNIA with gain $G_{LNIA} = 100$.

The measurement resolution is next calculated from a large set of simulated $V_X(P)$, at a single and known value of the pressure P and for a large set of offset V_{off} simulating a resistance drift $\delta R_m = -3\%R_2 \rightarrow +3\%R_2$ or a reference voltage drift $\delta V_ref = -3\%V_{ref} \rightarrow +3\%V_{ref}$. The mean value of the relative error made in the pressure measurement (i.e. $std(P_X(V))/P$) gives the estimated measurement resolution. Resolution curves are compared together with the best possible resolution performance expected with this post processing method (i.e. when the standard deviation of the subtracting point used in the common mode rejection is null). They are shown in "Fig. 9".

A first result is that the resolution of the pressure measurement is strongly independent upon the offset voltage V_{off} in

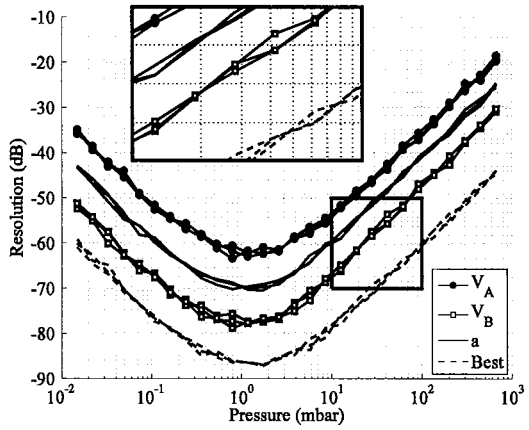

Fig. 9. Resolution of V_A, V_B, and a from (18) versus pressure for a large set of V_{off}. Inset: Magnification of the squared area which clearly shows that the measurement error is strongly independent of the offset value but depends on the offset rejection method.

case of both measurement signal $V_A(P)$ or $V_B(P)$ as seen in "Fig. 9". This demonstrates that the use of the micro-Pirani gauge's transient response is an efficient way to separate the steady state resistance variation of the gauge from a large set of unexpected offset voltage. In other words, the transient response processing provides a powerful means to enhance the correctness of the pressure measurement of the micro-Pirani gauge.

Next, the correctness of the measurement being achieved, the resolution is enhanced by 17 dB at least when the transient response of the micro-Pirani gauge is identified using a low order, low-pass filter ARMA modeling compared to a rough - but achieving - common mode rejection, as can be seen of "Fig. 9". This level of improvement is clearly in the order of what theoretically expected by (22).

Another result which was most unexpected could be unambiguously observed in "Fig. 6". First $1/\beta$ is pressure dependent. Second, it features a substantially shifted range of measurement of the Micro-Pirani gauge, with respect to the traditional monitoring of the micro-Pirani gauge, which only uses $\delta R_{1_{steady}}$. The range of measurement and the maximum sensitivity of the sensor are shifted to the atmospheric pressure by more than one decade. Thanks to (17) which is of the form of the computation of an Exponential Moving Average (EMA) step response, it can be shown that

$$\frac{1}{\beta(P)} \cong \frac{(a(P)+1)}{Fs} \tag{23}$$

so that the parameter a calculated by the *Steiglitz-McBride* algorithm could be a natural candidate for a direct measurement of the pressure. Furthermore, a pressure measurement based on $a(P)$ only would spare the computation of both $V_{ARMA}[n]$ and its mean value. However $a(P)$ does not feature a measurement resolution as good as $V_B(P)$, as seen in "Fig. 9".

It is important to notice that the value of a is by principle strongly independent upon the offset and upon $\delta R_{1_{steady}}$. However it depends on the sample frequency.

This very behavior of the transient response of our micro-Pirani gauge might not be confused with the observation reported by [7], whose substantial announcement was that the time constant of the transient response of a *macro*-Pirani gauge is increasing (i.e. $\partial(1/\beta)/\partial\log(P) < 0$) inside the 30 mbar to 1000 mbar range, which has not been observed with our micro-Pirani gauge, mostly because the gaseous layer thickness of the Pirani-gauge used by [5] is 16 mm thick.

V. Conclusion

This paper has investigated a digital post-processing suitable for the transient response analysis of a micro-Pirani pressure sensor. Based on electrical simulation and experimental results, several of the key features of the latter have been illustrated, that are recalled as a conclusion:

1) Robust to temperature and process variations,
2) Low-power operation,
3) Fast time processing,
4) Nearly maximal resolution.

The pressure measurement based on the time constant of the sensor's transient signal has been investigated. It provides a range of measurement significantly shifted towards the atmospheric pressure with regards to that of a traditional measurement with a micro-Pirani gauge. The time constant can be trustfully evaluated by an ARMA identification of the transient signal.

The heating step, the recording and the post-processing of the digital data can easily be achieved by a low-cost microcontroller.

References

[1] M. Doms, A. Bekesch, and J. Mueller, "A microfabricated pirani pressure sensor operating near atmospheric pressure," *J. Micromech. Microeng.*, vol. 15, no. 8, pp. 1504–1510, 2005.

[2] R. Puers, S. Reyntjens, and D. De Dbruyker, "The nanopirani – an extremely miniaturized pressure sensor fabricated by focused ion beam rapid prototyping," *Sensors Actuat. A*, vol. 97, no. 98, pp. 208–214, Apr. 2002.

[3] K. Khosraviani and A. M. Leung, "The nanogap pirani – a pressure sensor with superior linearity in an atmospheric pressure range," *J. Micromech. Microeng.*, vol. 19, no. 4, pp. 900–903, Mar. 2009.

[4] F. Santaga, J. F. Creemer, E. Iervolino, L. Mele, A. W. van Herwaarden, and P. M. Sarro, "A tube-shaped pirani gauge for low detection limit with small footprint," *J. Microelectromech. Syst.*, vol. 20, no. 3, pp. 676–684, May 2011.

[5] M. Boujama, B. Alandry, S. Hacine, L. Latorre, F. Mailly, and P. Nouet, "A low interface circuit for resistive sensor with digital offset compensation," in *Proc. IEEE Circuits Syst. Int. Symp.*, May 2010, pp. 3092–3095.

[6] L. Hebrard, F.-B. Kammerer, and F. Braun, "A chopper stabilized biasing circuit suitable for cascaded Wheatstone-bridge-like sensors," *IEEE Trans. Circuit Syst.*, vol. 52, no. 8, pp. 1653–1665, Aug. 2005.

[7] W. Jitchin and S. Ludwig, "Dynamical behavior of the pirani sensor," *Vacuum*, vol. 75, no. 2, pp. 169–176, Jul. 2004.

[8] M. Özisik, *Boundary Value Problems of Heat Conduction*. New York: Dover, 1968.

[9] P. Strica and T. Söderström, "The Steiglitz-McBride identification algorith revisited – convergence and accuracy aspect," *IEEE Trans. Autom. Control*, vol. 26, no. 3, pp. 712–717, Jun. 1981.

Olivier Legendre received the M.S. degree in sensor, measure, and instrumentation from École Supérieure de Physique et de Chimie Industrielles de la Ville de Paris, Paris, France, in 2009. He is currently pursuing the Ph.D. degree in microelectronics at the Université Paris-Sud, Paris.

He founded Legendre Electrique Devices in 2007, which is a start-up company that commercializes energy saving street light bulbs. His current research interests include thermal microelectromechanical systems sensors.

Hervé Bertin was born in Paris, France, in 1986. He received the B.S. degree from University Pierre and Marie Curie, Paris, in 2007, and the M.S. degree from the Université Paris-Sud, Paris, in 2009, where he is currently pursuing the Ph.D. degree in microtechnology.

His current research interests include optical and mechanical design of MOEMS, and process integration and development of tunable Fabry-Perot interferometer arrays for multispectral imaging.

Olivier Garel was born in Paris, France, in 1980. He received the M.S. degree in applied chemistry and Ph.D. degree in industrial processes engineering from the Université Paris-Sud, Paris, in 2005 and 2009, respectively.

Since 2005, he has been with the Institute of Fundamental Electronics, Université Paris-Sud in collaboration with NXP Semiconductors, Caen, France, involved in research on fabrication processes and characterization of porous silicon micro-devices for high-sensitivity measurement of moisture inside microelectromechanical systems packages.

Ming Zhang received the M.S. degree in telecommunications and signal processing from Xidian University, Xi'an, China, in 1985, and the Ph.D. degree in electrical engineering from the Université Paris-Sud, Paris, France, in 1994.

She was an Associate Professor with the Beijing Information Engineering Institute, Beijing, China, from 1985 to 1989, and the École Nationale Supérieure d'Electronique, d'Informatique, et de Radiocommunications de Bordeaux, Paris, from 1994 to 2001. Since 2002, she has been an Associate Professor with the Université Paris-Sud, Paris. She holds a U.S. patent on voltage-to-voltage converters. Her current research interests include the study of analogue nonvolatile memories, integrated voltage-to-voltage converters, and microelectromechanical systems sensors.

Dr. Zhang was a recipient of the IBM France Prize in 2003 for her contribution in voltage-to-voltage converters.

Hervé Mathias received the Ph.D. degree in microelectronics from École Centrale de Lyon, Lyon, France, in 1996, for his research on analog integrated circuits layout automation.

Since 1996, he researched the design of parallel integrated architectures for image processing with Henri Poincare University, Nancy, France. He is currently an Associate Professor with the Institute of Fundamental Electronics, Université Paris-Sud, Paris, France, where he is researching modeling, design, and testing of microelectromechanical systems sensor and their associated electronics.

Souhil Mergherbi received the Ph.D. degree in microelectronics from the Université Paris-Sud, Paris, France, in 1992.

He is currently a Professor of electronic engineering with the Université Paris-Sud, where he is a Member of Administration Council, and the Director of the University Institute of Technology, Cachan, France. His current research interests include microelectromechanical systems and its associated electronics.

Jérôme Juillard was born in Nice, France, in 1973. He received the Ingénieur Centralien degree from École Centrale de Paris, Châtenay-Malabry, France, in 1995, and the Ph.D. degree in physical acoustics from University Denis Diderot, Paris, France, in 1999.

He is currently a Professor with the Department of Signal Processing and Electronic Systems, Supélec, Gif-sur-Yvette, France. His current research interests include nanoelectromechanical systems and microelectromechanical systems sensors, reduced-order modeling, nonlinear dynamics, and parameter estimation methods.

Frédérick Mailly was born in Montmorency, France, in 1974. He received the Ph.D. degree in electronics from the University of Montpellier, Montpellier, France, in 2002.

From 1999 to 2004, he researched design, manufacturing, and modeling of thermal microsensors and bulk-acoustic-wave resonators with the Center of Electronics and Micro-Optoelectronics, Montpellier University. From 2004 to 2005, he was with the Montpellier Laboratory of Computer Science, Robotics, and Microelectronics, Montpellier University. Since 2005, he has been an Assistant Professor with the Polytechnic Engineering School of Montpellier University. His current research interests include microelectromechanical systems design for manufacturing and testability.